MAP signal reconstruction with non regular grids

João M. Sanches* Jorge S. Marques

IST/ISR, Torre Norte, Av. Rovisco Pais, 1049-001, Lisbon, Portugal

Abstract. The estimation of a scalar function f using a regular grid has been extensively used in image analysis. This amounts to approximate f by a linear combination of known basis functions. However, this approach is usually not efficient. This paper proposes a more efficient algorithm, based on the use of a non regular grid, which achieves better accuracy with less basis functions. Experimental results are provided to illustrate the performance of the proposed technique.

1 Introduction

The representation of continuous functions using linear interpolation of a given set of basis functions is a common procedure in several areas [1–3]. Non-uniform grids are used in a large number of applications, e.g., finite elements mathematics, image format conversion, surface representation in computer graphics and curve re-sampling. Usually these non uniform sampled problems are converted to uniform sampled problems by re-sampling the data. For instance [6] presentes an algorithm to re-sample data between arbitrary grids using an intermediary rectangular regular grid.

This procedure can be performed by using some optimality criterion, e.g. least squares reconstruction (LSR) error [4, 5] . The main problem in these conversion operations is the representation error introduced when a given continuous or discrete function is represented using a different set of basis functions.

In this paper we will adopt a different strategy: instead of converting a non regular grid problem into a regular one we will start with a regular grid and change its geometry in order to minimize a given energy function.

We aim to represent a continuous function, $f(x)$, estimated from noisy observations at non uniform positions x_i. This function is represented as a linear combination of basis functions which vary during the estimation process. The proposed method uses the MAP criterion to estimate the coefficients associated to basis functions and to estimate its positions. This approach allows to estimate the basis functions as well as its coefficients.

* corresponding author: João Sanches, IST/ISR, Torre Notre, Av. Rovisco Pais, 1049-001 Lisboa, Portugal, Email:jmrs@alfa.ist.utl.pt, Phone:+351 21 8418195

2 Problem Formulation

Let $f(x)$ be a scalar function and $V = \{(y_i, x_i)\}$ a set of M observations, where y_i are noisy observations of $f(x)$ taken at locations x_i. The goal is the estimation of $f(x)$ from the data V, by minimizing an energy function.

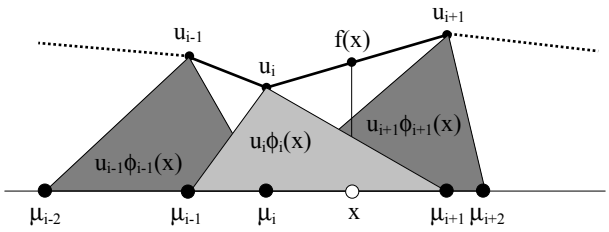

Fig. 1. Function representation with a non regular grid.

2.1 $f(x)$ definition

It is assumed that the $f(x)$ belongs to a class of admissible functions defined in an interval $\Omega \subset R$, i.e., $f : \Omega \longrightarrow R$. Furthermore, it is assumed that the set of admissible functions is a finite dimension vector space F with unknown basis function, $\phi_i : \Omega \longrightarrow R$, belonging to a given class of functions. Each function $f \in F$ can be expressed as a linear combination of the basis functions,

$$f(x) = \Phi(x)^T U \tag{1}$$

where $\Phi(x) = [\phi_1(x), \phi_2(x), ..., \phi_N(x)]$ is a vector of basis functions and $U = [u_1, u_2, ..., u_N]$ is a $N \times 1$ vector of coefficients.

Piecewise linear basis functions are used as shown in Fig.1. The shape and regions of support of the basis function are different depending on the distances between the μ_i's, where the μ_i parameter is the position of the maximum of the basis function ϕ_i (see Fig. 1). Therefore, the value of $f(x)$ at an arbitrary location x in the interval $[\mu_i, \mu_{i+1}]$ is obtained by interpolating the coefficients u_i and u_{i+1}, as follows

$$f(x) = u_i \frac{x - \mu_{i-1}}{\mu_i - \mu_{i-1}} + u_{i+1} \frac{\mu_{i+1} - x}{\mu_{i+1} - \mu_i} \tag{2}$$

All the basis functions are initialized with the same shape and at equally spaced positions, that is, forming a uniform regular grid, where $\mu_i = \min(x) + i * (\max(x) - min(x))/(N-1)$ with $0 \leq i \leq N-1$.

2.2 Observation model

In this paper we assume that the observations are corrupted by Gaussian additive noise, $\eta_i \sim N(0, \sigma^2)$, with zero mean and standard deviation σ, i.e.,

$$y_i = f(x_i) + \eta_i \tag{3}$$

Assuming that the observations are independent this leads to the log likelihood function

$$l_y = C - \frac{1}{2\sigma^2} \sum_{j=1}^{M} (y_j - f(x_j))^2 \tag{4}$$

where $C = -\frac{1}{2} \log (2\pi\sigma^2)$.

2.3 Prior

The assumption that $f(x)$ is band limited, makes it possible to model the vector $U = \{u_i\}$ as a Markov Random Field, described by a Gibbs distribution. This approach introduces correlation between the values of neighboring nodes [7], which is expected for band limited signals.

Furthermore, in this paper, changes on the shape of the basis functions are performed. By changing the positions μ_i's of the basis functions we will maximize a given objective function. Constraints should be introduced to avoid the collapsing of all nodes in a one single point. Therefore, the vector $\Xi = \{\mu_i\}$ is also modeled as a Markov Random Field described by Gibbs distribution.

In this paper it will be used first order Markov Random Fields described by Gibbs distributions [7] with quadratic potential functions with parameters α and β for the vectors U and Ξ respectively, i.e.,

$$P(U) = \frac{1}{Z_u} e^{-\alpha \sum_{i=2}^{N} (u_i - u_{i-1})^2} \tag{5}$$

$$P(\Xi) = \frac{1}{Z_\mu} e^{-\beta \sum_{i=2}^{N} (\mu_i - \mu_{i-1})^2} \tag{6}$$

where Z_u and Z_μ are the partition functions associated to $P(U)$ and $P(\Xi)$ respectively.

The estimation of U and Ξ is performed by using the MAP criterion,

$$\begin{aligned} \hat{U} &= arg \max_{U} \log (P(Y|U, \Xi) P(U) P(\Xi)) \\ \hat{\Xi} &= arg \max_{\Xi} \log (P(Y|U, \Xi) P(U) P(\Xi)) \end{aligned} \tag{7}$$

2.4 Energy

The optimization problem defined by the equations (7) can be solved by minimizing the following energy function

$$E(U, \Xi) = -l_y - l_u - l_\mu \tag{8}$$

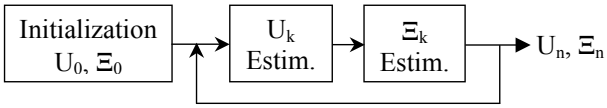

Fig. 2. Optimization process.

with respect to U and with respect to Ξ, where $l_u = \log(P(U))$ and $l_\mu = \log(P(\Xi))$. Replacing l_y, l_u and l_μ we obtain

$$E(U,\Xi) = C + \frac{1}{2\sigma^2}\sum_{j=1}^{M}(y_j - f(x_j))^2 - \sum_{i=1}^{N}(\alpha(u_i - u_{i-1})^2 + \beta(\mu_i - \mu_{i-1})^2) \tag{9}$$

3 Optimization

The minimization of (9) is performed based on two steps: 1)optimization with respect to U and 2)optimization with respect to Ξ, as displayed in Fig.2. These two steps alternate during the iterative process until the convergence is achieved. In each step, the optimization is performed by using the ICM algorithm [8], where the energy function is minimized with respect to each unknown, keeping all the other constant. Ξ is initialized with a regular grid in Ω where $\mu_1 = x_{min}$ and $\mu_N = x_{max}$. Concerning the coefficients U, they are first initialized with a constant value, the mean of $\{y_i\}$.

The minimization of $E(U,\Xi 1)$ with respect to the parameters is performed by finding its stationary point with respect to u_i and μ_i, i.e., by solving the following equations

$$\begin{aligned}\frac{\partial E(U,\Xi)}{\partial u_i} &= 0\\ \frac{\partial E(U,\Xi)}{\partial \mu_i} &= 0\end{aligned} \tag{10}$$

Using the fixed point algorithm we obtain

$$\begin{aligned}u_i^{n+1} &= \frac{1}{2\alpha\sigma^2}\sum_{j=1}^{M}(y_j - f(x_j))\phi_i(x_j) + \bar{u}_i\\ \mu_i^{n+1} &= \frac{1}{2\beta\sigma^2}\sum_{j=1}^{M}(f(x_j) - y_j)\frac{df(x_j)}{d\mu_i} + \bar{\mu}_i\end{aligned} \tag{11}$$

where $u_i = (u_{i-1} + u_{i+1})/2$, $\mu_i = (\mu_{i-1} + \mu_{i+1})/2$ and

$$\frac{df(x)}{d\mu_i} = \begin{cases} \frac{(u_{i-1}-u_i)(x-\mu_{i-1})}{(\mu_i-\mu_{i-1})^2} & \mu_{i-1} < x \leq \mu_i \\ \frac{(u_i-u_{i+1})(\mu_{i+1}-x)}{(\mu_{i+1}-\mu_i)^2} & \mu_i < x \leq \mu_{i+1} \\ 0 & otherwise \end{cases}$$

During the optimization process μ_1 and μ_N, are not updated, preventing the collapse of the nodes into a single position. In fact, it is important to note that the prior associated to Ξ favors the approximation of the nodes due to the use of quadratic distances between consecutive node positions.

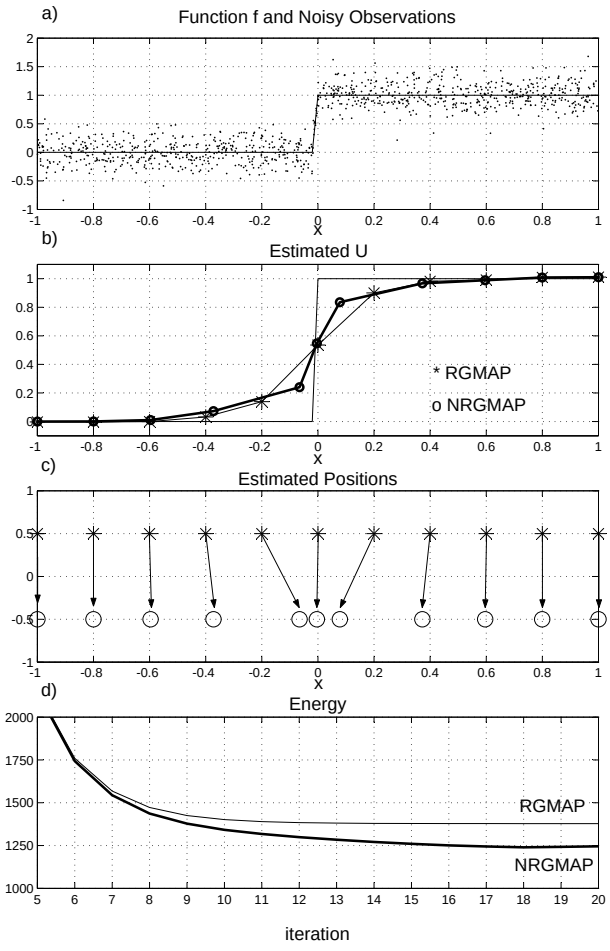

Fig. 3. Experiment with synthetic data. a)Original function and the observations. b)Estimated functions with the RGMAP (*) and NRGMAP (o). c)Node locations. d)Energy function.

4 Experimental results

In this sections we will present experiments using synthetic data and real data.

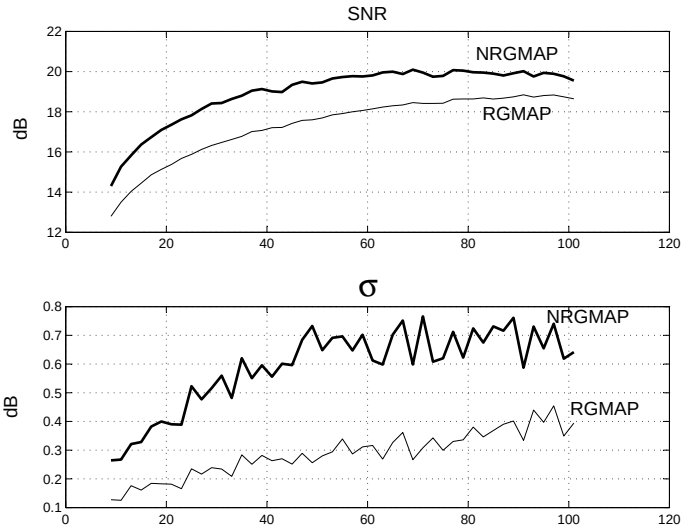

Fig. 4. Monte Carlo tests. Mean and standard deviation of the SNR obtained with 40 experiments for each number of nodes between N=11 and N=111.

4.1 Synthetic data

The first experiment considers synthetic data. We have generated a set of 1000 points uniformly distributed in the interval $[-1, 1]$. The function $f(x)$, to be estimated, is a a step function with transition at $x = 0$. The observations, y_i, obtained at locations x_i are corrupted with additive Gaussian noise, with zero mean and standard deviation $\sigma = 0.2$ (see Fig.3.a)). The function $f(x)$ is defined using a linear combination of 11 basis functions.

The locations of the nodes associated to the basis functions are initialized as a regular grid, i.e., they are equally separated in the interval $[-1, 1]$. In a first experiment we have estimated only the coefficients u_i of the basis functions. In a second step we have jointly estimated the coefficients and the corresponding locations. Figs.3.b-d) show the results. Fig.3.b) shows the original function $f(x)$, the estimated function using the regular grid based MAP method (RGMAP), marked with asterisks, and the estimated function using the non regular grid based MAP method (NRGMAP), marked with circles. Fig.3.c) shows the final positions of the nodes for both methods, and Fig.3.d) shows the evolution of the energy function along the iterative process of estimation.

The NRGMAP method achieves lower values for the energy function ($E_{NRGMAP} = 1190$, $E_{RGMAP} = 1314$) and the nodes tend to concentrate at the transitions, as expected. The final result is clearly better.

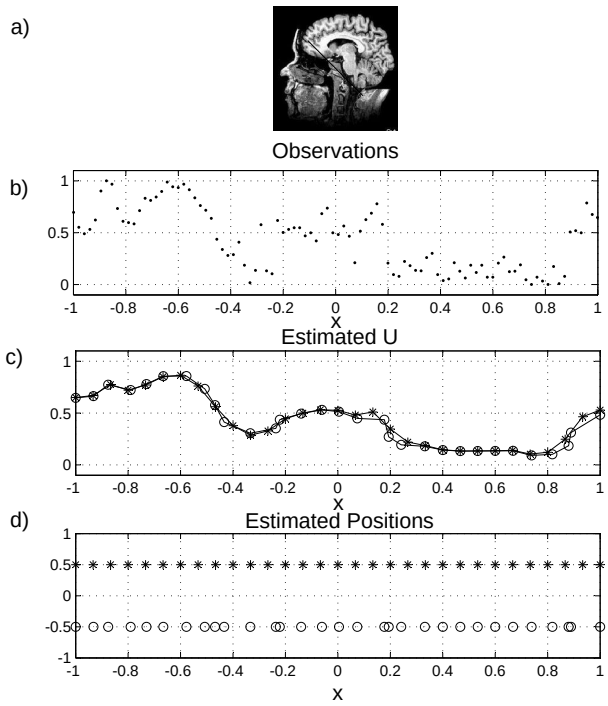

Fig. 5. Estimation of MRI profile: a) MRI image. b)Observations. c)Estimated functions. d)Node positions.

4.2 Monte Carlo tests

We have performed monte carlo tests, with the parameters used in the previous experiment, but with different number of nodes, starting with $N = 11$ and ending with $N = 111$. For each number of nodes we have performed 40 experiments and for each one we have computed the signal to noise ratio of the estimated function using both methods. The mean and standard deviation of the SNRs obtained in the 40 experiments were computed and the results are displayed in the Fig.4. These results show that the NRGMAP method always works better leading to a gain of approximated 2dB. This gain, however, decreases as the number of nodes increases, because when the number of nodes is large, the function is already well represented with a regular grid. The adjustments on the node positions, in this case, do not leads to relevant improvements in the representation of $f(x)$.

4.3 Real data

In a second experiment we show a 1D profile obtained from a MRI image of the brain (see Fig.5.a)). We have used this profile to estimated a scalar function describing the anatomy along the profile, using 31 basis functions. The results are displayed in Fig.5. Once again, lower values of the energy function are achieved using the NRGMAP method, meaning a function that better represents the observations, and the nodes tend to approximate in the regions where the function to be estimated presents faster variations.

5 Conclusions

In this paper we have presented an algorithm to estimate a function from noisy observations sampled at arbitrary positions in a given interval. The function is described as a linear combination of a finite number of basis functions where the corresponding locations are optimized using the MAP criterion. We have shown that this strategy of jointly estimating the coefficients and corresponding positions leads to better results than estimating only the coefficients of the linear combination. Our goal is to apply this strategy to higher order problem by deforming 2D or 3D grids in order to obtain better representation of the estimated function with the small number of nodes as possible.

Acknowledgment

This work was partially supported by FCT under project HEART 3D (SAPIENS).

References

1. T. Lehmann, C. Spitzer, Survey:Interpolation Methods in Medical Image Processing, IEEE Trans. on Medical Imaging, vol.18, no.11, November 1999.
2. P. Thvenaz, T. Blu, M. Unser, Interpolation Revisited, IEEE TMI, vol.19, no.7, July 2000.
3. A. Jonas, N. Kiryati, Digital Representation Schemes for 3D Curves, Pattern Recognition, 1803-1816, 1997.
4. H. Sederat, D.G. Nishimura, On the Optimality of the Gridding Recosntuction Algorithm, IEEE TMI, vol.19, no.4, April 2000.
5. M. Barrutia, T. Blu, M. Unser, Non-Uniform to Uniform Grid Conversion Using Least-Squares Splines, Proceedings of the Tenth European Signal Processing Conference (EUSIPCO'00), Tampere, Finland, September 4-8, 2000, vol. IV, pp. 1997-2000
6. V. Rasche et al., Resampling of Data Between Arbitrary Grids Using Convolution Interpolation, IEEE TMI, vol.18, no.5, May 1999.
7. S. Geman, D. Geman, Stochastic Relaxation, Gibbs Distributions, and the Bayesian Restoration of Images, IEEE PAMI, 721-741, November 1984.
8. J. Besag, On the Statistical Analysis of Dirty Pictures, J. R. Statist. Soc. B, vol.48, no. 3, pp. 259-302, 1986.